Preparation of Vanadium Nitride by Magnesiothermic Reduction of V_2O_3 in Nitrogen Atmosphere

YUE-DONG WU, GUO-HUA ZHANG, and KUO-CHIH CHOU

The development of a highly efficient and low-cost production process is instrumental for the wide application of vanadium nitride (VN). The strong affinity of vanadium with carbon and oxygen resulted in the significant difficulty to produce VN with a high purity. In this paper, a novel production route was proposed that involves the magnesiothermic reduction and nitration of vanadium (III) oxide (V_2O_3) in nitrogen atmosphere with the assistance of magnesium chloride ($MgCl_2$) in the temperature range of 948 K to 1073 K (675 °C to 800 °C). Compared with the traditional methods, there was no contamination of carbon. Meanwhile, oxygen content can be controlled to a low level. Furthermore, VN could be prepared at low temperatures within a short time, which was beneficial for decreasing the particle size of VN. The phase transition and morphological evolution of samples were analyzed by X-ray diffraction and Field-Emission Scanning Electron Microscopy, respectively. The experimental results showed that high temperature assisted in decreasing the residual oxygen content in VN but can decrease the specific surface area. Oxygen content of the obtained VN powder after reacting at 1073 K (800 °C) for 3 hours was 1.36 wt pct.

https://doi.org/10.1007/s11663-018-1388-3

I. INTRODUCTION

VANADIUM nitride (VN) is regarded as a highly promising material, owing to its excellent physical properties such as extreme hardness, high melting point, high-temperature stability (8.1×10^{-6} K^{-1}), and low thermal conductivity (11.3 W m^{-1} K^{-1}).[1–3] Considering these excellent properties, VN has been widely applied in various industrial fields, such as catalysis, superconducting devices, cutting tools.[4–6] Particularly, owing to its excellent activity and selectivity, VN has been used in catalytic hydroprocessing, including hydrodenitrogenation (HDN), hydrodesulfurization (HDS), and hydrodeoxygenation (HDO).

Currently, VN is primarily produced by the vacuum carbonitrothermic reduction process. In this process, V_2O_3 is reduced with carbon under vacuum condition at 1373 K to 1773 K (1100 °C to 1500 °C) and then nitrided to produce VN. The reactions can be described as follows:

$$V_2O_3 + (2x+3)C \rightarrow 2VC_x + 3CO (x<1) \quad [1]$$

$$VC_x + (y/2)N_2 \rightarrow VC_xN_y. \quad [2]$$

The main disadvantages of the carbonitrothermic reduction process are that it is energy intensive and has a high cost due to some specific technical requirements during the high-temperature reaction process. Besides, the high contents of residual carbon and oxygen are also problematic. Therefore, a large number of investigations have been conducted recently to produce VN with a low cost and a high purity. Tripathy *et al.*[7] prepared vanadium nitride by heating a mixture of vanadium pentoxide and graphite powder in a flowing nitrogen atmosphere. The oxygen and nitrogen contents were controlled to 2.5 and 3 wt pct, respectively. Qian *et al.*[8] reported that VN nanocrystals can be synthesized by the decomposition followed by the nitridation of precursor NH_4VO_3 in an autoclave with metallic Na as flux at 723 K to 873 K (450 °C to 600 °C), as shown by Eq. [3],

$$NH_4VO_3 + 3Na \rightarrow VN + 3NaOH + 0.5H_2. \quad [3]$$

Kapoor *et al.*[9] prepared VN with a high surface area (90 m^2/g) by temperature programmed reduction and nitridation of V_2O_5 in ammonia atmosphere. Qian *et al.*[10] had successfully synthesized nanocrystalline VN by the reaction between VCl_4 and $NaNH_2$ at room temperature. Hong *et al.*[11] directly prepared VN nanopowders *via* decomposition of gas phase vanadium

YUE-DONG WU, GUO-HUA ZHANG, and KUO-CHIH CHOU are with the State Key Laboratory of Advanced Metallurgy, University of Science and Technology Beijing, Beijing 100083, China. Contact e-mail: ghzhang0914@ustb.edu.cn
Manuscript submitted April 12, 2018.
Article published online August 15, 2018.

oxytrichloride ($VOCl_3$) under $N_2/Ar/H_2$ microwave plasma condition. Besides, some other methods were also proposed, such as reactive magnetron sputter deposition,[12] ammonolysis of metal chlorides or sulfides,[13–15] and nitridation of metal vanadium.[2]

Based on the Ellingham diagram, Na, Ca, and Mg are the possible reductants to reduce V_2O_3. Although the reduction ability of Mg is not as strong as that of Ca, it is still effective to reduce V_2O_3. Furthermore, Mg is the cheapest reductant among them. Fang *et al.*[16–18] also successfully prepared high-quality Ti metal by magnesiothermic reduction of TiO_2 with the assistance of molten salt in recent years. Therefore, a novel route to prepare vanadium nitride by magnesiothermic reduction and nitridation of V_2O_3 was proposed in this work. Owing to the extreme chemical affinity of Mg with oxygen, oxygen content in VN can be reduced to a low level. Furthermore, by this route, carbon can be avoided. Because of the extremely exothermic behavior of magnesiothermic reduction reaction, $MgCl_2$ was added to decrease the local temperature as well as improve the reaction kinetics. After reaction, the byproduct MgO could be removed by acid leaching, and the produced $MgCl_2$ solution was dried to generate $MgCl_2$ salt which could be re-used.

II. EXPERIMENTAL PROCEDURES

A. *Raw Materials*

The main chemicals used in this research, including hydrochloride acid, anhydrous $MgCl_2$, KCl, and Mg powder, were obtained from Sinopharm Chemical Reagent Beijing Co., Ltd, China. V_2O_3 powder (> 95 wt pct) was purchased from Alfa Aesar, England. The average powder size of V_2O_3 and Mg were 2.492 and 135.702 μm, respectively.

B. *Experiments*

V_2O_3 powder, anhydrous $MgCl_2$, and Mg metal powder were weighed and mixed uniformly. The $MgCl_2/V_2O_3$ molar ratio was about 4, while the Mg/V molar ratio was 1.5, 2.25, or 3. Then, the mixture was placed into a Mo crucible, which was accommodated into the constant-temperature zone of a vertical tube furnace using $MoSi_2$ rods as the heating elements. The furnace temperature was raised to the desired value [948 K to 1073 K (675 °C to 800 °C)] at a heating rate of 5 K/min and held for 3 hours. After that, the sample was cooled down to room temperature gradually before being taken out from the furnace. During the entire process, N_2 gas was introduced into the furnace with a flow rate of 500 mL/min. The schematic diagram of the experimental apparatus is described and shown in Figure 1. After high-temperature reaction, MgO was removed by leaching the as-produced sample in 1M HCl at 298 K (25 °C) for 3 hours. Then, the samples were filtered and washed several times with deionized water. The wet powder was then dried in the oven and collected for detection. The flowchart of the process is described in Figure 2. During the whole process, except for the molten salt, only high-purity V_2O_3 (> 95 wt pct, with the other component of high-valence vanadium oxide) and Mg (> 99 wt pct) powders were used. Therefore, the carbon content of the final product should be very low. In order to study the distributions of VN and MgO particles, some samples only washed by deionized (DI) water were also studied. The temperature higher than the melting point of Mg (921 K) can enhance the deoxygenation kinetics. But, if the temperature was too high, it would lead to a large evaporation loss of Mg. $MgCl_2$ salt was added to decrease the local temperature. Therefore, the temperature should be higher than the melting point of $MgCl_2$ (991 K). In order to prepare VN powder at a low temperature, $MgCl_2$-50 wt pct KCl eutectic salt with a melting point of about 760 K (487 °C) was used in some experiments, and the corresponding reaction temperatures were 948 K and 973 K (675 °C and 700 °C), respectively.

The phase composition of sample was examined *via* X-ray diffraction (XRD, TTR III; Rigaku Corporation, Tokyo, Japan) using Cu Kα radiation in the range of $2\theta = 10$ to 90 deg with a scanning rate of 10 deg min^{-1}. The morphology was characterized using the combination of field-emission scanning electron microscopy (FE-SEM, JSM-6701F, Japan) and energy dispersive spectroscopy (EDS). Selected area electron diffraction (SAED) and high-resolution transmission electron microscopy (HRTEM) images were captured by using a Tecnai G2 microscope. The residual oxygen content in the final products was determined by the thermal conductimetric method after fusion in an inert gas (GB/T 24583.2-2009). The surface area was measured by the Brunauer Emmett Teller method (BET, AUTOSORB-IQ2; Quanta chrome, Boynton Beach, Florida, USA). The powder size was measured by Laser particle size distribution analyzer (LMS-30, Tokyo, Japan).

III. RESULTS

A. *Phase Transition*

The magnesiothermic reduction and nitridation reaction of V_2O_3, as described above, involved a series of phase transformations. Figures 3(a) through (c) show the XRD patterns of the obtained samples prepared under different conditions. For the as-prepared sample after reacting at 1023 K (750 °C) with the Mg/V molar ratio of 3, as can be seen from Figure 3(a), all the peaks were assigned to $MgCl_2$, MgO, and VN. When the sample was leached in DI water, $MgCl_2$ phase was removed and the sample only consisted of MgO and VN. After further leaching in HCl solution, it can be seen that all the diffraction peaks were assigned to VN phase. The total reactions can be described as follows:

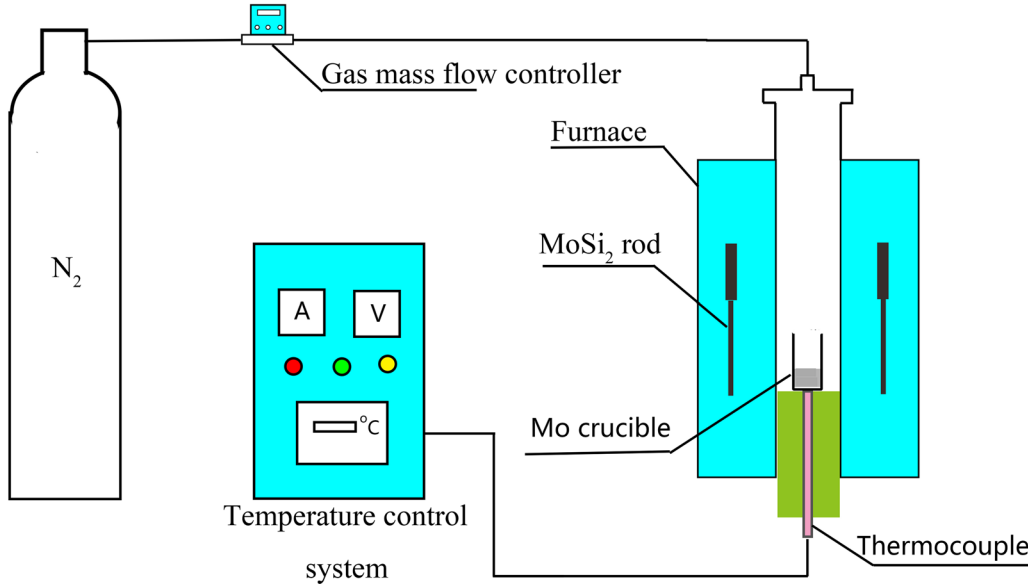

Fig. 1—Schematic diagram of the experimental apparatus.

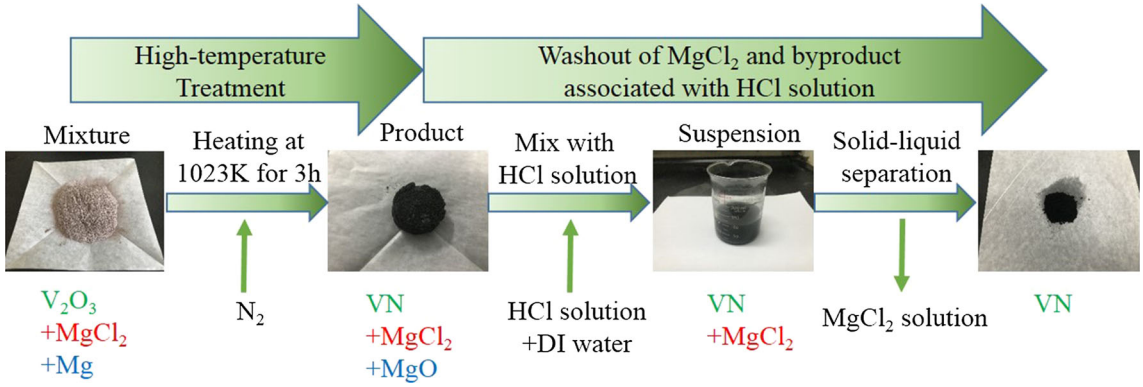

Fig. 2—Flowchart of the production process.

$$V_2O_3 + 3Mg + N_2 = 2VN + 3MgO \quad [4]$$

$$2HCl + MgO = MgCl_2 + H_2O \quad [5]$$

$$V_2O_3 + MgO = MgV_2O_4. \quad [6]$$

Figure 3(b) presents the XRD patterns of VN powder prepared at 1023 K (750 °C) with different Mg/V molar ratios. When Mg/V molar ratio was greater than 2.25, all the characteristic peaks belonged to VN phase. In contrast, when Mg/V molar ratio was 1.5, a small amount of MgV_2O_4 was detected because the content of Mg was not sufficient to reduce all the oxides owing to its evaporation loss. The residual V_2O_3 reacted with MgO to produce MgV_2O_4 as described by Eq. [6].

Figure 3(c) presents the XRD patterns of VN powder prepared at 998 K, 1023 K, 1048 K, and 1073 K (725 °C, 750 °C, 775 °C, 800 °C) with the Mg/V molar ratio of 2.25. The corresponding enlarged peaks splitting at 2θ = 37 deg are given in Figure 3(d). From it, it was evident that nearly all peaks were identified as VN in the temperature range of 998 K to 1073 K (725 °C to 800 °C). Moreover, it was observed that the characteristic peaks of VN were slightly shifted to a smaller diffraction angle as the temperature was increased. This indicated that the lattice constant of VN phase increased which resulted from the decrease of residual oxygen content. It was widely recognized that a continuous solid solution of V(N, O) could be formed easily because of the similar crystalline structures of VO and VN. Thus, it was very difficult to completely remove oxygen from VN. With increasing the temperature, the deoxygenation rate enhanced gradually and more oxygen atoms (atomic

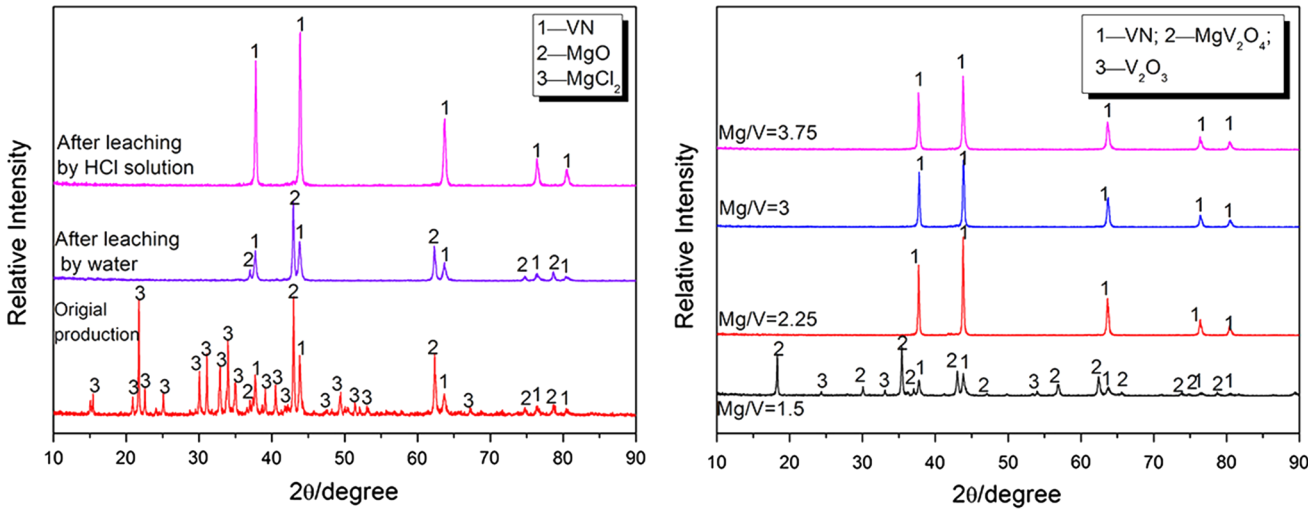

(a)

(b)

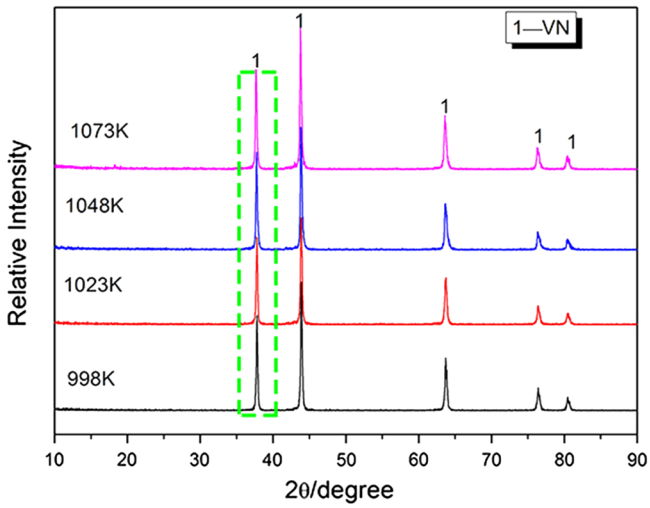

(c)

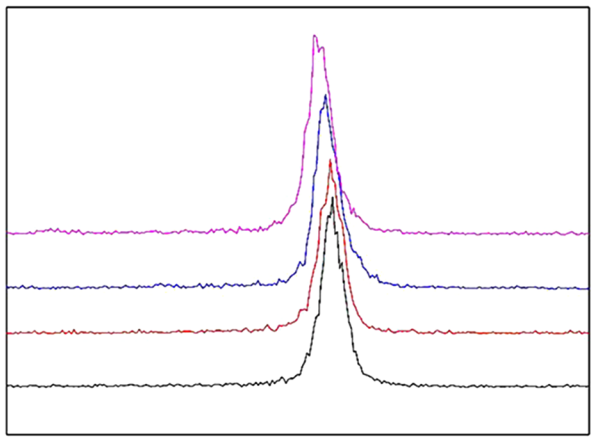

(d)

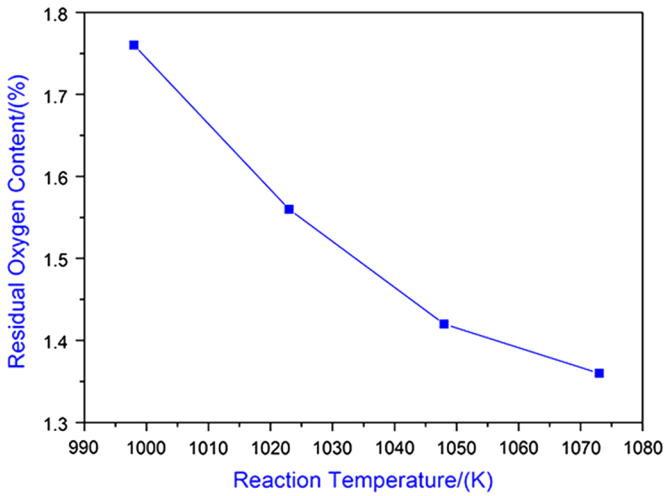

(e)

Fig. 3—(*a*) XRD patterns of the originally reduced and further treated samples obtained at 1023 K (750 °C) at the Mg/V molar ratio of 3; (*b*) XRD patterns of VN powder prepared at 1023 K (750 °C) at different Mg/V molar ratios; (*c*) XRD patterns of VN powder prepared at the Mg/V molar ratio of 2.25 at different temperatures; (*d*) the enlarged peaks splitting at $2\theta = 37$ deg in (c); (*e*) the residual oxygen content of VN powder shown in (c).

radius 0.074 nm) in VN lattice would be replaced by nitrogen atoms (atomic radius 0.075 nm). In order to confirm this phenomenon, the residual oxygen of VN prepared at different temperatures was measured as well (Figure 3(e)). It can be seen that the corresponding residual oxygen decreased from 1.76 to 1.36 wt pct as the reaction temperature increased. These findings agreed well with the XRD patterns. Therefore, the high temperature was beneficial for improving the quality of VN.

B. *Microstructure*

Figure 4 illustrates the morphological evolution of VN particles in the temperature range of 948 K to 1073 K (675 °C to 800 °C). From Figure 4(a), it can be seen that most of the VN particles were roughly spherical with the size of approximately 400 nm. Meanwhile, the particle also exhibited a porous structure. When the temperature was increased to 973 K (700 °C), as shown in Figure 4(b), the particle size became slightly larger. Although the spherical shape was unchanged, the porosity decreased. The decrease of porosity was much more evident at 998 K (725 °C) as shown in Figure 4(c). With a further increase of the temperature, two kinds of morphologies were found. Both of them were identified as VN phase by EDS. As indicated in Figures 4(d) and (e) which corresponded to samples obtained at 1023 K and 1048 K (750 °C and 775 °C), respectively, the size of big particles was larger than 1 μm. These smooth particles may result from the sintering phenomenon among particles. The specific surface area of VN particles prepared at these temperatures decreased significantly relative to those prepared at the low temperatures. Finally, when the temperature was increased to 1073 K (800 °C) as shown in Figure 4(f), most particles had a large size and smooth surface. The specific surface area of VN powder prepared at different temperatures was measured and the results are shown in Figure 5. The specific surface area decreased from 29.167 to 1.163 m^2/g with the increasing temperature, which agreed well with the morphological evolution.

Figures 4(g) and (h) present SEM image and EDS results of the sample prepared at 998 K (725 °C) after leaching by DI water. The EDS analysis showed the byproduct MgO was surrounded by VN particles. According to previous researches,[16,19] during the magnesiothermic reduction, MgO was formed and distributed tightly with the other products, which prevented the physical contacts and sintering among different particles, as well as the self-densification of the particles. When the sample was leached in HCl solution, MgO particles were removed, which resulted in the porous VN particles as shown in Fig. 4(b).

C. *TEM Characterization*

TEM image in Figure 6(a) presented the morphology of VN powder prepared at 1023 K (750 °C). It can be seen that at 1023 K (750 °C), most of the fine particles experienced considerable sintering. EDS results shown in Figure 6(b) further confirmed that the obtained powder was VN. The SAED pattern (Figure 6(c)) showed two directions corresponding to the [111] and [220] reflections of VN. In HRTEM image (Figure 6(d)), the lattice fringes were clearly visible with a spacing of 0.237 nm, which corresponded to the [111] plane of VN. The spacing was slightly smaller than the standard value of the [111] plane (0.238 nm),[20] which may be caused by the existence of few oxygen in VN. Furthermore, according to the formula $d = a/\mathrm{sqrt}(h^2 + k^2 + l^2)$ for a cubic system, the lattice constant (a) of VN particles prepared at 1023 K (750 °C) was calculated to be 4.105 Å.

IV. DISCUSSION

A. *Adiabatic Temperature Calculation*

The magnesiothermic reduction and nitridation reaction of V_2O_3 (Eq. [4]) is a strongly exothermic reaction. In order to evaluate the real reaction temperature, the adiabatic temperature (Tad), *i.e.*, the theoretical temperature calculated under the adiabatic condition, was computed using the following formula[21]:

$$-\Delta H^{\theta}_{1023} = \int_{1023}^{T_{tr}} nCp(\text{products})\mathrm{d}T + n\Delta H_{tr} + \int_{T_{tr}}^{T_{ad}} nCp(\text{products})\mathrm{d}T, \quad [7]$$

where ΔH^{θ}_{1023} is the difference between the molar enthalpy of formation of the products and the raw materials at 1023 K (750 °C); n is the mole number of each product and Cp is the molar heat capacity. Any phase transformation during the heating should be considered in the calculations. Thus, in Eq. [7], T_{tr} is the transformation temperature and ΔH_{tr} is the molar enthalpy of this transformation process. According to Eqs. [4] and [7], the adiabatic temperature could be calculated and the effect of $MgCl_2$ addition on the adiabatic temperature is shown in Figure 7. The thermodynamic data used to calculate the adiabatic temperature were obtained by FactSage 6.4.[22] It was observed from Figure 7 that the adiabatic temperature gradually decreased with the increase of the $MgCl_2/V_2O_3$ molar ratio. When the molar ratio was in the range of 3.85 to 15.6, the adiabatic temperature was kept at 1631 K (1358 °C), owing to the vaporization of $MgCl_2$ salt. Further increasing the molar ratio of $MgCl_2$ to V_2O_3, the adiabatic temperature decreased gradually. In our experiments, the molar ratio of $MgCl_2$ to V_2O_3 was close to 4. Therefore, in this case, the adiabatic temperature was 1631 K (1358 °C). However, owing to the heat exhaustion, the actual temperature must be lower than 1631 K (1358 °C).

B. *Thermodynamic Analysis*

As indicated above, VN powder can be prepared by a magnesiothermic reduction and nitridation reaction of V_2O_3 at low temperatures. It was mentioned that the overall reaction can be described by Eq. [4]. Strictly, VN was generated by two steps: (1) magnesiothermic reduction reaction of V_2O_3; (2) nitridation reaction, as described by Eqs. [8] and [9]:

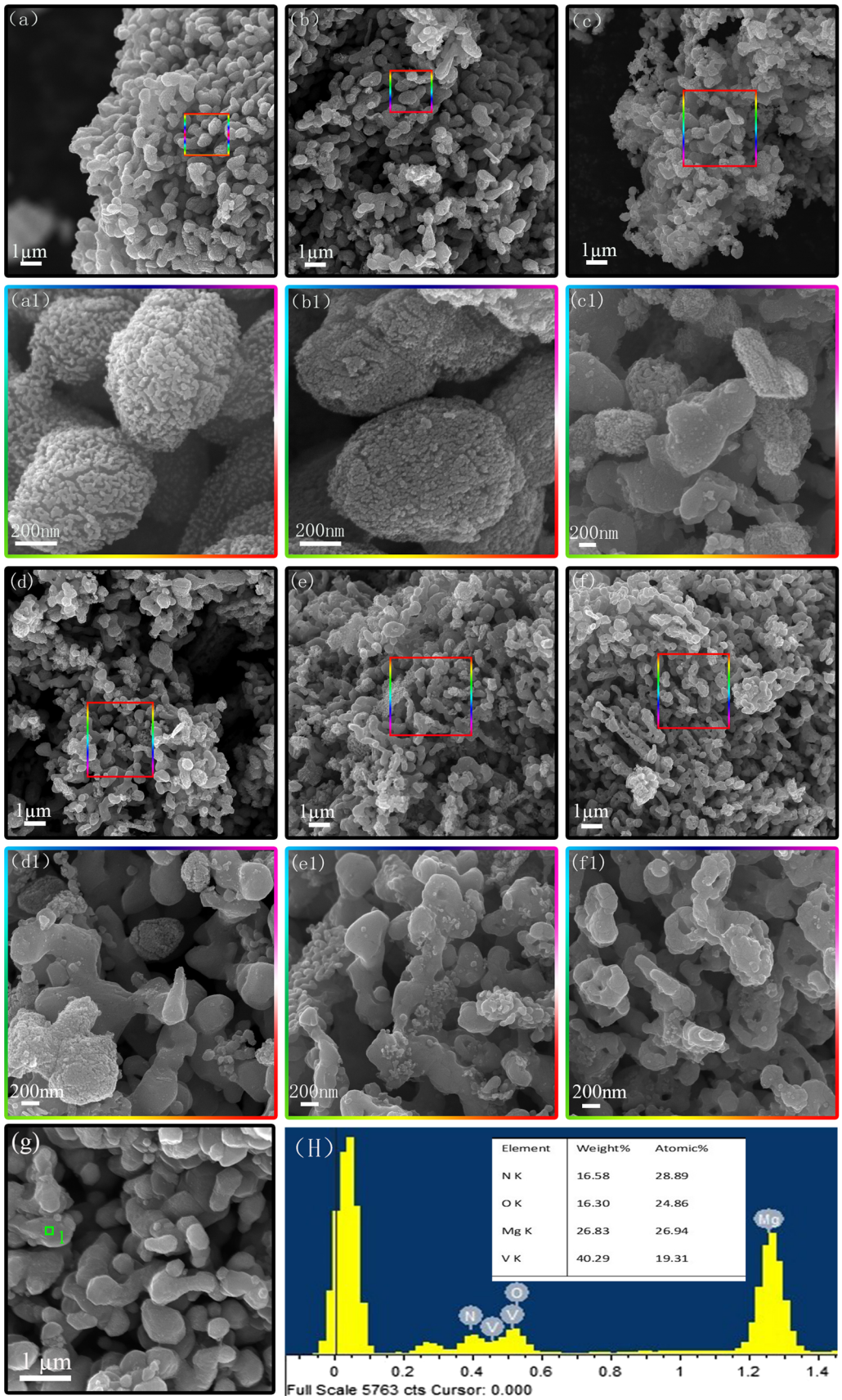

Fig. 4—(*a*) through (*f*) SEM images of the final products prepared with the Mg/V molar ratio of 2.25 at different temperatures ((a) 948 K (675 °C), (b) 973 K (700 °C), (c) 998 K (725 °C), (d) 1023 K (750 °C), (e) 1048 K (775 °C), (f) 1073 K (800 °C)); (a1) through (f1) a partial enlarged part of graph (a) through (f); (*g*) SEM image of the reduced sample prepared at 998 K after leaching by DI water; (*h*) EDS of the sample pointed in (g).

$$V_2O_3 + 3Mg = 2V + 3MgO$$

$$\Delta G_1 = \Delta G^\theta + RT\ln K = -602151.8 + 86.21T \quad [8]$$

$$2V + N_2 = 2VN$$

$$\Delta G_2 = \Delta G^\theta + RT\ln K = -214807.5 + 83.22T + RT\ln(1/P_{N_2}/P^\theta). \quad [9]$$

ΔG^θ for Eqs. [8] and [9] was calculated using FactSage 6.4. At temperature lower than 1631 K (1358 °C), ΔG_1 and ΔG_2 were always negative. This indicated that at the experimental temperatures, Eqs. [8] and [9] can occur easily from the viewpoint of thermodynamics.

In order to further analyze the process of magnesiothermic reduction and nitridation reactions of V_2O_3 in a nitrogen atmosphere, the predominant area phase diagram in V-O-Mg-N system at 1631 K (1358 °C) is calculated and shown in Figure 8. Considering the continuous introduction of high-quality N_2, the partial pressure of N_2 was close to 1 atm. From Figure 8, it

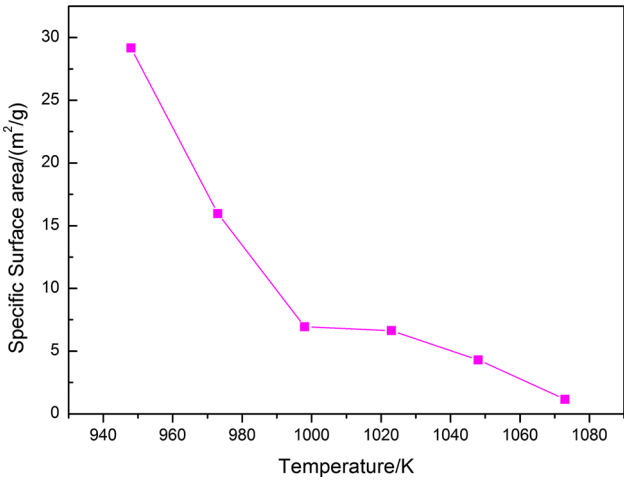

Fig. 5—Specific surface area of VN powder prepared at different temperatures.

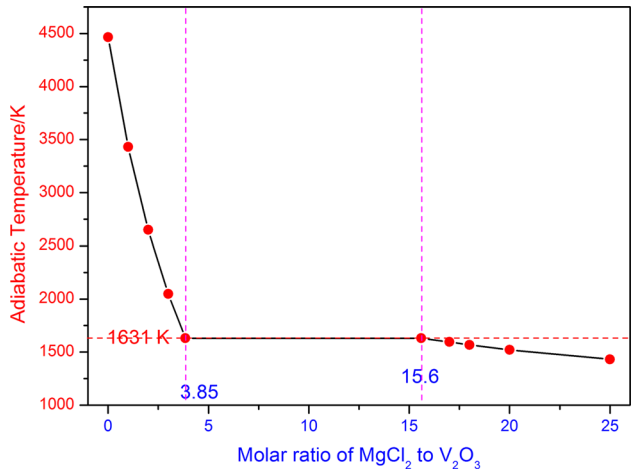

Fig. 7—Effect of $MgCl_2$ addition on the adiabatic temperature of the Reaction [4].

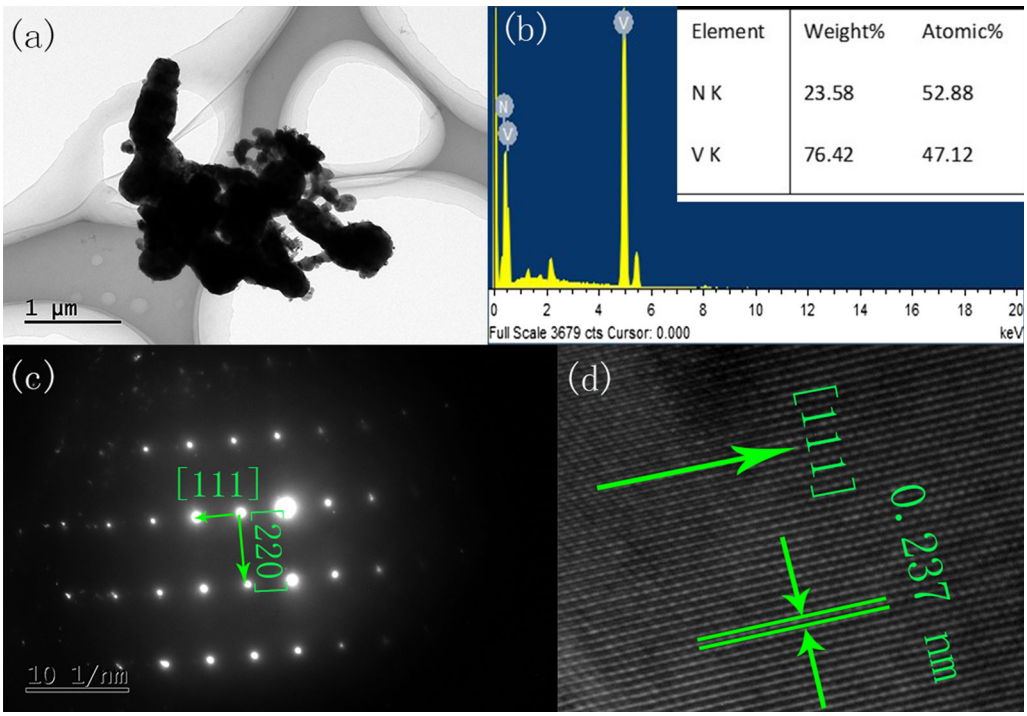

Fig. 6—(*a*) TEM image of VN particles prepared at 1023 K (750 °C); (*b*) EDS spectrum; (*c*) SAED pattern; (*d*) HRTEM image.

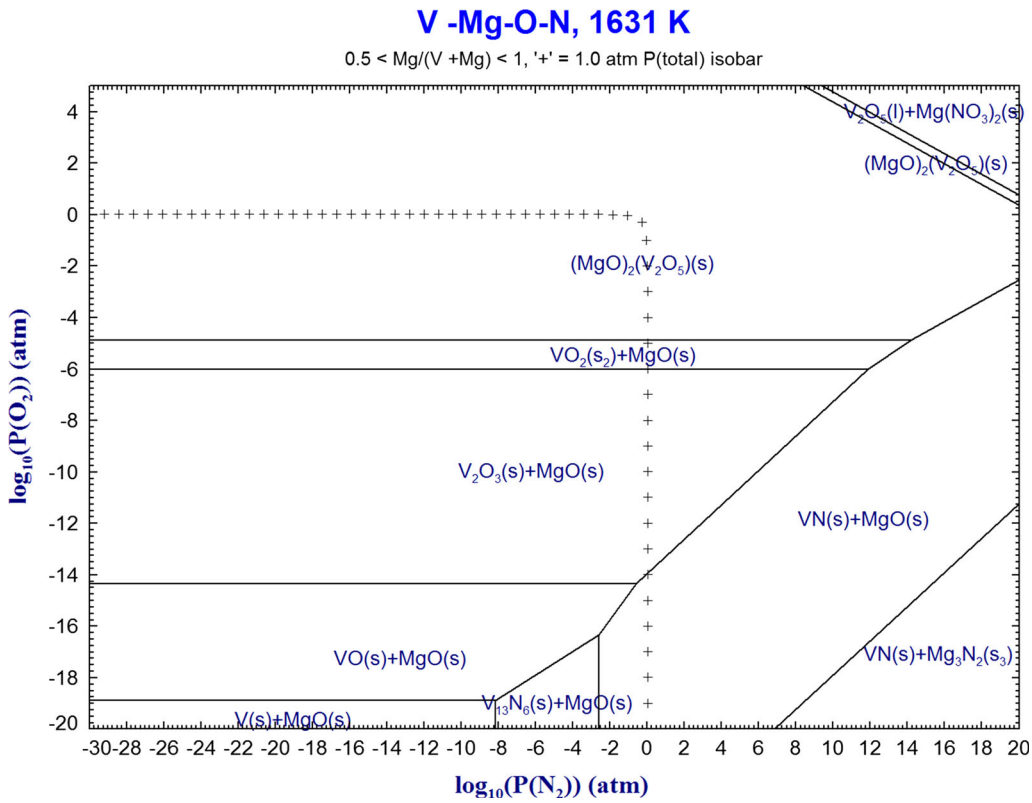

Fig. 8—Predominant area phase diagram in V-O-Mg-N system at 1631 K (1358 °C).

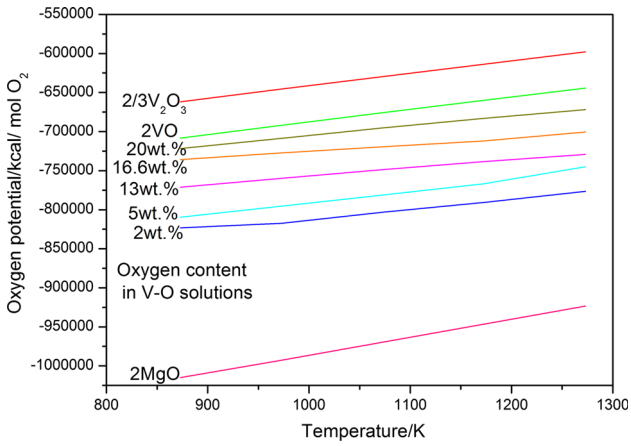

Fig. 9—Ellingham diagram of MgO, V_2O_3, VO, and V-O solutions.

could be seen that the stable phase was sensitive to the partial pressure of O_2. Only when the partial pressure of O_2 was lower than 10^{-14} atm, VN and MgO were the stable phases.

It is well known that Ellingham diagram presents the change of the standard Gibbs free energy for oxidation reaction of different elements (oxygen potential) as a function of the temperature. The lower the oxygen potential, the stronger the reducibility of the corresponding metal will be. For different reactions, the oxidation reaction and the corresponding standard Gibbs free energy change should be described based on 1 mol oxygen gas:

$$2x/y\mathrm{M} + \mathrm{O_2} = 2/y\mathrm{M}_x\mathrm{O}_y \ (\mathrm{M} = \mathrm{V},\ \mathrm{Mg}) \qquad [10]$$

$$\Delta G^{\theta} = -RT\ln K^{\theta} = -RT\ln\frac{1}{P_{\mathrm{O_2}}/P^{\theta}}. \qquad [11]$$

Therefore, Ellingham diagram of MgO, V_2O_3, VO, and V-O solutions could be calculated and is shown in Figure 9. The thermodynamic data used to calculate the Ellingham diagram were obtained from FactSage 6.4 and some related literature.[22–25] Figure 9 presents the oxygen potentials of MgO, V_2O_3, VO, and V-O solutions. MgO was more stable than V_2O_3 and VO. Moreover, when oxygen dissolved in the lattice of V metal to form a V-0.6wt pctO solid solution, its oxygen potential was still higher than that of MgO. This implied that Mg was a stronger reductant and could reduce the oxygen content in V metal to a very low value in the temperature range of 873 K to 1273 K (600 °C to 1000 °C) from the viewpoint of thermodynamics. However, the oxygen content of VN powder prepared at different temperatures after reacting for 3 hours was in the range of 1.76 to 1.36 wt pct. The thermodynamic result was lower than the actual oxygen content in VN powder. This may result from the slow rate of the deep deoxygenation reaction of low oxygen-vanadium solid solution. To confirm this, VN

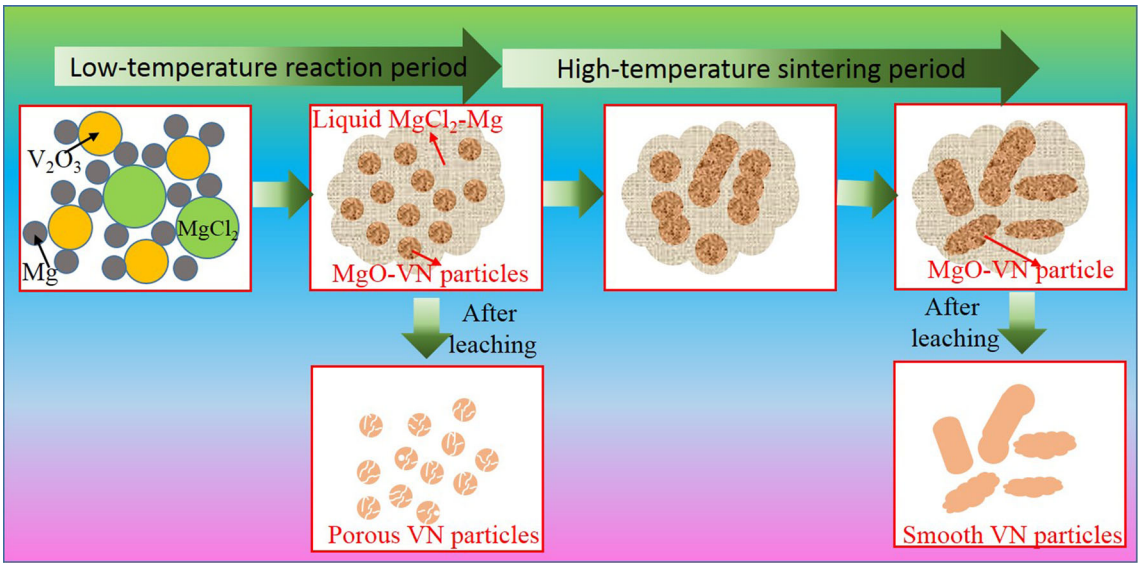

Fig. 10—Mechanism diagram about the preparation of VN powder.

powder prepared at 1023 K (750 °C) after reacting for 6 hours was obtained. Compared with the VN reaction for 3 hours, the oxygen content decreased from 1.56 to 1.44 wt pct. Therefore, a longer reduction time can further increase the purity of VN powder.

C. *Reaction Mechanism*

Based on the above experimental observations and thermodynamic analyses, the underlying mechanism of the current process to prepare VN was speculated and is illustrated in Figure 10. To simplify the analyses, the particle shapes of all raw materials are assumed to be spherical. Mg, V_2O_3, and $MgCl_2$ were mixed uniformly and contacted each other. As the temperature was increased to the target value, Mg and $MgCl_2$ became liquid state. Then, the reaction between V_2O_3 and Mg started quickly to produce V. Since N_2 was continuously introduced to the system, VN particles began to nucleate and grow based on Eq. [9]. Moreover, MgO was formed and distributed tightly with the VN particles. When the temperature was low, the sintering was not intense. Thereby, after leaching MgO by acid, VN particles with a porous structure were obtained. However, at high temperature, the sintering driving force among different VN particles increased significantly. The growth of VN particles was mainly in the form of neck-sintering between particles, which contributed to the formation of large and smooth chunks as shown in Figure 4(f). Herein, the positive effect of $MgCl_2$ salt should be noted. During the reaction process, $MgCl_2$ became liquid state and did not take part in the reaction, but it can facilitate the mass transfer of the reductant, which improved the kinetic rate of the reaction.[18]

V. CONCLUSION

High-quality VN was prepared successfully by magnesiothermic reduction and nitridation reactions of V_2O_3 with the assistance of $MgCl_2$. Compared with the traditional methods, the introduction of carbon could be avoided by this route, and the residual oxygen content could be controlled to a low level. The experimental results showed that high temperature was beneficial for decreasing the oxygen content in VN, but can decrease the specific surface area. At 948 K (675 °C), the prepared VN particles were approximately spherical, and had a porous structure as well as a large specific surface area.

ACKNOWLEDGMENTS

The authors gratefully acknowledge the financial support from the National Natural Science Foundation of China (51734002 and 51725401).

REFERENCES

1. H.O. Pierson: *Handbook of Refractory Carbides and Nitrides: Properties, Characteristics, Processing and Applications*, Noyes Publications, New York, 1996.
2. Z. Zhao, Y. Liu, H. Cao, J. Ye, S. Gao, and M. Tu: *J. Alloy. Compd.*, 2008, vol. 464, pp. 7580.
3. H. Kwon, A. Moon, W. Kim, and J. Kim: *Ceram. Int.*, 2018, vol. 44, pp. 284755.
4. G.W. Wiener and J.A. Berger: *JOM*, 1955, vol. 7, pp. 36068.
5. J. Zhao, B. Liu, S. Xu, J. Yang, and Y. Lu: *J. Alloy. Compd.*, 2015, vol. 651, pp. 78592.
6. S. Ramanathan, C.C. Yu, and S.T. Oyama: *J. Catal.*, 1998, vol. 173, pp. 1016.
7. P.K. Tripathy, J.C. Sehra, and A.V. Kulkarni: *J. Mater. Chem.*, 2001, vol. 11, pp. 69195.
8. Z. Yang, P. Cai, L. Chen, Y. Gu, L. Shi, A. Zhao, and Y. Qian: *J. Alloy. Compd.*, 2006, vol. 420, pp. 22932.
9. R. Kapoor and S.T. Oyama: *J. Solid State Chem.*, 1992, vol. 99, pp. 30312.
10. L.Y. Chen, Y.L. Gu, L. Shi, Z. Yang, J. Ma, and Y. Qian: *Solid State Commun.*, 2004, vol. 132, pp. 34346.
11. Y.C. Hong, D.H. Shin, and H.S. Uhm: *Mater. Chem. Phys.*, 2007, vol. 101, pp. 3540.
12. X. Chu and S.A. Barnett: *J. Vac. Sci. Technol. A*, 1996, vol. 14, pp. 312429.

13. J. Pieterá Dekker and P.J. ávan der Put: *J. Mater. Chem.*, 1994, vol. 4, pp. 68994.
14. Y.G. Li, L. Gao, J.G. Li, and D.S. Yan: *J. Am. Ceram. Soc.*, 2002, vol. 85, pp. 129496.
15. P.S. Herle, M.S. Hegde, N.Y. Vasathacharya, S. Philip, M.V.R. Rao, and T. Sripathi: *J. Solid State Chem.*, 1997, vol. 134, pp. 12027.
16. Y. Zhang, Z.Z. Fang, Y. Xia, P. Sun, B. Van Devener, M. Free, and S. Zheng: *Chem. Eng. J.*, 2017, vol. 308, pp. 299310.
17. Z.Z. Fang, S. Middlemas, J. Guo, and P. Fan: *J. Am. Chem. Soc.*, 2013, vol. 135, pp. 1824851.
18. Y. Zhang, Z.Z. Fang, Y. Xia, Z. Huang, H. Lefler, T. Zhang, and J. Guo: *Chem. Eng. J.*, 2015, vol. 286, pp. 51727.
19. Y.T. Yuan, W. Li, H.L. Chen, Z.Y. Wang, X.B. Jin, and G.Z. Chen: *Faraday Discuss.*, 2016, vol. 190, pp. 8596.
20. K. Becker and F. Ebert: *Z. Phys.*, 1925, vol. 31, pp. 26872.
21. M. Sharifitabar, J. Vahdatikhaki, and M. Haddad: Sabzevar*Int. J. Refract. Met. Hard Mater.*, 2014, vol. 47, pp. 93101.
22. C.W. Bale, A.D. Pelton, W.T. Thompson, G. Eriksson, K. Hack, P. Chartrand, S. Decterov, I.-H. Jung, J. Melanc and S. Petersen: *FactSage, version 6.4, Thermfact and GTT-Technologies*, 2013.
23. E. Fromm and R. Kirchheim: *J. Less. Common Met.*, 1972, vol. 26, pp. 40306.
24. I.A. Vasil'eva and A.N. Seregin: *Zh. Fiz. Khim.*, 1982, vol. 56, pp. 161821.
25. Z. Cao, S. Li, W. Xie, G. Du, and Z. Qiao: *Calphad*, 2015, vol. 51, pp. 24151.